Nuclear Physics A457 (1986) 401-412
North-Holland, Amsterdam

SUBBARRIER FUSION IN MEDIUM HEAVY NUCLEI

J.Q. WU and G.F. BERTSCH

National Superconducting Cyclotron Laboratory, Department of Physics and Astronomy, Michigan State University, East Lansing, Michigan 48824, USA

Received 20 December 1985
(Revised 1 April 1986)

Abstract: An excellent description of the fusion excitation function in the system Ti+Zr is obtained in a model coupling collective surface excitations to the relative motion. For heavier systems that require an "extra push" for fusion, the coupled channel model reproduces the relative enhancements associated with different isotopes, but does not describe the absolute cross section well. In solving the coupled channel problem, we found that the adiabatic representation is very useful when many channels are allowed.

1. Introduction

Subbarrier fusion has been studied intensively in recent years [1]), both experimentally and theoretically. This has been partially motivated by the search for superheavy elements, which can be made by fusion at the lowest possible energies. There is also intrinsic interest in the question of how tunnelling takes place in the large dimensional space of the many-particle wavefunction. It is well known that the one-dimensional barrier penetration model underestimates subbarrier fusion, by orders of magnitude in heavy systems. There one has to go beyond the potential barrier model to reproduce the data. This was demonstrated in work by Balantekin *et al.* [2]), in which an effective one-dimensional potential was extracted directly from the fusion data. The potential obtained for heavy systems has a inner edge with a negative slope which is unphysical. Thus one cannot fit the data by manipulating the parameters or forms of one-dimensional potentials.

Internal excitation is known to play an important role in the subbarrier region. The coupling to the lowest excitations of nuclei was considered by Rhoades-Brown *et al.* [3]) who found clear dependence of the subbarrier fusion enhancement on the collectivity of the nuclei. However, their calculation did not give enough enhancement for energies very far below the barrier. To get a good description into the far subbarrier region, more channels must be included than are visible in the direct excitations from the ground state. Additional channels are included in a simple way in the zero-point motion model (ZMP), which uses a harmonic oscillator for the deformation degree of freedom [4]). This model successfully describes the fusion excitation function using transition strengths close to the observed strengths for the low collective excitations [5]). However, the model assumes that the oscillator

frequency is small compared to the tunnelling frequency, which is only justified for very soft nuclei [6]). In this paper, we shall examine the role of deformation on the fusion, using a large channel space of harmonic excitations but avoiding the ZPM approximation of small frequency. Calculations using a model with a similar hamiltonian structure have been made by Krappe *et al.* [7]). However, they have a quite different interpretation for their internal oscillator degree of freedom, associating it with fluctuations in the coordinates of a neck joining the nuclei rather than in the shape of the nuclei in isolation. The neck coordinates will be important degrees of freedom in heavy collision systems that have touching nuclei at the barrier top. For the lighter systems we consider, below the extra-push threshold, the nuclei are separated at the barrier top and deformations in shape better describes fluctuations in configuration.

Another degree of freedom we do not consider at all in this work is particle transfer. If deformations are strongly suppressed, as in the magic nucleus system $^{16}O + ^{208}Pb$, the subbarrier enhancement may be mostly due to particle transfer [8]). If the nuclei are softer, particle transfer is only expected to play a role in special situations with positive Q values [9]).

In the next section we discuss the coupled-channel equations and the methods we use to solve them. The parameters of the calculations are described in sect. 3. The comparison with experiment is given in sect. 4.

2. Coupled equations

Many intrinsic degrees of freedom may be excited during the collision of heavy ions. For subbarrier fusion these degrees of freedom have to be separated out from the optical potential and treated explicitly because their influence on the fusion depends sensitively on the energy below the Coulomb barrier. The set of coupled radial equations in a typical problem has the structure

$$\left(\frac{\hbar^2}{2M}\frac{\partial^2}{\partial r^2} + V(r) - E\right)\Psi(r) = 0\,, \tag{1}$$

where $\Psi(r)$ is a n-dimensional vector (n is the total number of channels explicitly treated in the calculation). Each component $\Psi_i(r)$ is the wave function in channel i and $V(r)$ is a $n \times n$ potential matrix. Its off-diagonal matrix elements are the couplings, while its diagonal elements are the internuclear potential in different channels. The E is a diagonal matrix with the energies of the relative motion in different channels as its diagonal elements.

Numerically, however, the many-channel coupling calculation is difficult, especially in the case where more than one mode of intrinsic excitation is included in the model space. Several techniques can be applied to solve the coupled equations. The method of iterations with Padé approximants has been used by several authors [3]). This is successful in many cases, but for subbarrier fusion the computations are

very lengthy and good convergence may not be obtained when many channels are strongly coupled. Another method is to invert the matrix connecting inner and outer boundary conditions [6]). Then convergence is not a problem. But the numerical precision can quickly become a limiting factor when the number of channels increases. Below the barrier the matrix to be inverted has elements which differ by orders of magnitude. This is because the wave functions in various channels are exponential functions with different decay lengths. The precision limitation may be overcome by dividing the barrier region into several intervals. The transmission matrix is constructed for each segment and the complete transmission is obtained from the product. We had to use this refinement for some models with a very large number of channels, but for the cases studied in this work it was not necessary.

Another technique, used in ref. [7]) makes use of the adiabatic representation. The coupled-channel basis is transformed to diagonalize $V(r)$ at each point. Then eq. (1) becomes

$$\left(\frac{\hbar^2}{2M} D(r) \frac{\partial^2}{\partial r^2} D^{-1}(r) + D(r) V(r) D^{-1}(r) - E\right) D(r) \Psi(r) = 0 , \tag{2}$$

where $D(r)$ is the transformation matrix and $D(r) V(r) D(r)^{-1}$ is diagonal. The basis is truncated to a few states with the lowest energies. If the space is truncated to a single state and the derivatives of D^{-1} are dropped in the kinetic energy operator, we obtain the well-known adiabatic approximation. This limit is employed in the subbarrier fusion calculations of Tanimura *et al.* [10]). We shall compare the accuracy of various truncations in sect. 3 below.

3. Details of the calculations

Our formulation of the surface coupling model follows that of Esbensen [4]). The internal degrees of freedom are described by a harmonic oscillator hamiltonian in an internal coordinate s. The coupling to the radical coordinate is through the ion-ion potential, which is taken to be of the form

$$V(r, s) = \frac{Z_1 Z_2 e^2}{r} + \frac{3 Z_1 Z_2 e^2 R_1 s}{5 r^3} + V_0 \frac{R_1 R_2}{R_1 + R_2} \frac{1}{\sqrt{\pi}} \int_{(r - R_1 - R_2 - \Delta R - s)/(4a/\pi)}^{\infty} e^{-x^2} \, dx . \tag{3}$$

We use an error function form for the ion-ion potential for convenience in the calculations. The geometric parameter R_i and a are determined from an ion-ion potential fit to elastic scattering data [11]),

$$R_i = 1.233 A_i^{1/3} - 0.98 A_i^{-1/3} , \qquad a = 0.63 \text{ fm} . \tag{4}$$

The depth of the potential is determined by requiring that the maximum force reproduce the proximity potential [11]),

$$V_0 = -31.67 \text{ MeV} . \tag{4a}$$

The coupled-channel equations will be solved for an incoming wave boundary condition at the radius where the entrance channel potential has its minimum. We treat ΔR in eq. (3) as an adjustable parameter to fit the fusion above the barrier. For Ti+Zr systems, ΔR is 0.35 fm. It is 0.40 fm for all other systems we considered. It should be mentioned that potential parameters are far from unique as far as fusion is concerned. At most two parameters are determined by the above-barrier cross section, namely the barrier height and the barrier position. Other sets of V_0, a, ΔR give the same fit and the same coupled-channel results below the barrier.

The Coulomb excitation in a heavy system has an important effect on the fusion cross section [12]), partially cancelling the effect of the nuclear excitation. We include Coulomb excitation with the second term in eq. (3). The two-dimensional model does not include effects of angular momentum transfer, but these should be small because the systems are heavy.

The oscillator hamiltonian $H_{\rm in}(s)$ is specified by the frequency $\hbar\omega$ and by σ, the r.m.s. amplitude of the internal coordinate in the ground state. The Schrödinger equation for the system is the two-dimensional equation

$$\left(\frac{\hbar^2}{2M}\frac{\partial^2}{\partial r^2}+H_{\rm in}(s)+V(r,s)\right)\Psi(r,s)=E\Psi(r,s)\,. \tag{5}$$

The coupled equation is obtained by expanding $\psi(r,s)$ as

$$\psi(r,s)=\sum_{i=1}^{N}\psi_i(r)\phi_i(s)\,, \tag{6}$$

where the ϕ's are oscillator states. Integrating out s, we obtain eq. (1) with matrix elements given by

$$V_{ij}(r)=\int \mathrm{d}s\,\phi_i(s)\,V(r,s)\phi_j(s)\,. \tag{7}$$

The internal hamiltonian $H_{\rm in}(s)$ should be chosen to reproduce the energy and transition strength of the lowest excitations of the nuclei. For a single nucleus, the relation of σ to the $B(EL\downarrow)$ of a transition is given by eq. (11) in ref. [4]):

$$\sigma_\lambda=\frac{R}{Z(\lambda+3)}\left((2\lambda+1)\frac{B(\mathrm{E}\lambda\downarrow)}{B_w(\mathrm{E}\lambda)}\right)^{1/2}. \tag{8}$$

The excitation of both nuclei may be treated with a single coordinate s if the energies are degenerate; in that case the effective amplitude of the deformation is related to the individual amplitudes by

$$\sigma=\sqrt{\sigma_1^2+\sigma_2^2}\,. \tag{9}$$

Eq. (9) will also be applied in cases where the excitation energies are not degenerate and both excitations are important. The lower of two energies will be used if the difference is small. Otherwise we take the average of two energies as oscillator

TABLE 1

The parameters of surface vibrations deduced from the measurement of low-lying states

Nucleus	Energy of the first excited state (MeV)	σ(fm)
^{90}Zr	2.18	0.16
^{94}Zr	0.91	0.16
^{50}Ti	1.55	0.25
^{46}Ti	0.889	0.49
^{81}Br	0.7	0.36
^{93}Nb	0.9	0.22

For odd nuclei they are averages of those of two neighbor even-even nuclei. The σ's (standard deviations) are calculated according to eq. (8).

energy. As we shall see this procedure gives parameters for H_{in} that describe the reaction ^{50}Ti + ^{90}Zr very well below the barrier. For the softer system ^{46}Ti + ^{90}Zr, the method gives too much subbarrier fusion and we treat σ as an adjustable parameter.

For an odd nucleus the $\hbar\omega$ and σ of the collective excitation are hard to extract from the spectroscopic data. We expect the values of these parameters lie between those of two neighbor even-even nuclei. The values of ω and σ obtained in this way are given in table 1. Table 2 gives the values of the parameters used in describing the fusion data.

In our calculations, 5 or 6 channels are required to accurately calculate the cross section when it is down to the 100 μb level. The conventional matrix inversion method with double-precision arithmetic has sufficient accuracy in this case. However, if the adiabatic representation is used, only 2 or 3 channels are needed in the basis. This is demonstrated in table 3, comparing the S-wave fusion cross sections for ^{50}Ti + ^{90}Zr under various truncations. The first 5 states in the entrance channel representation define the space. One would expect the results to be independent of representation if the full space is used. From the last row of the table we

TABLE 2

The parameters of surface vibrations used in the fusion cross section calculations of figs. 1-5

Reaction	$\hbar\omega$ (MeV)	σ(fm)
^{50}Ti + ^{90}Zr	1.55	$0.3 = \sqrt{0.25^2 + 0.16^2}$
^{46}Ti + ^{90}Zr	0.918	(0.39)
^{46}Ti + ^{93}Nb	0.9	$0.45 = \sqrt{0.22^2 + (0.39)^2}$
^{50}Ti + ^{93}Nb	$1.2 = \frac{1}{2}(0.9 + 1.5)$	$0.32 = \sqrt{0.22^2 + 0.25^2}$
^{81}Br + ^{90}Zr	(0.9)	(0.32)
^{81}Br + ^{94}Zr	0.9	$0.36 = \sqrt{(0.32)^2 + 0.16^2}$

The parameters in parentheses were obtained by fitting to the data. The rest were taken or calculated from table 1.

TABLE 3

Calculated $^{50}Ti + ^{90}Zr$ S-wave fusion cross sections at a c.m. energy of 100 MeV as a function of number of channels in the model space in different representations with parameters given by eq. (4), eq. (4a) and table 2

No. of channels	Representation		Adiabatic approximation
	entrance	adiabatic	
1	0.03 μb	18.4 μb	46.7 μb
2	0.98 μb	6.65 μb	
3	3.45 μb	6.45 μb	
5	5.61 μb	6.51 μb	

see that this is not quite the case; the definition of an incoming wave boundary condition depends somewhat on the representation. The adiabatic truncations show that a 2-state truncation has converged, although a 1-state truncation is quite poor. The adiabatic approximation, which is the 1-state truncation with the entrance channel kinetic operator, works poorly here. In the entrance channel representation several states are needed. If a factor of 2 is tolerable in the accuracy, the space can be truncated to 3 channels. This is consistent with the findings of Takigawa *et al.* [13]).

4. Results and discussions

The fusion excitation function for $^{50}Ti + ^{90}Zr$ calculated from the model is compared with experiment [14]) in fig. 1. As one can see, the fusion is underestimated by the conventional barrier penetration model (thick continuous curve). The predicted fusion is factor of 60 too low at $E_{c.m.} = 100.6$ MeV, when the cross section is fit in the barrier region. The fusion is enhanced by coupling the excitation of the first excited state to the relative motion (dot-dashed curve). But it is still underestimated by a factor of 3 at the lowest energy. One is naturally led to expect that the contributions from higher intrinsic excitations would account for the difference. Unfortunately the parameters of the coupling of the higher excitations to the relative motion are hard to extract from the spectrum. However, if we approximate these excitations as pure harmonic vibrations, we get the full channel coupling results shown by the thin solid curve in the figure. The agreement below the barrier is very good in this approximation. The above-barrier fusion is slightly overpredicted by our model, though the $(Z^2/A)_{eff}$ of the system does not exceed the extra-push threshold [15]). We also show the prediction from ZPM. Although the orders of magnitude are right, the ZPM overpredicts the fusion of the $^{50}Ti + ^{90}Zr$ for energy far below the Coulomb barrier. Alternatively if the ZPM is fit to the data, then the potential barrier is too low at high energies [14]).

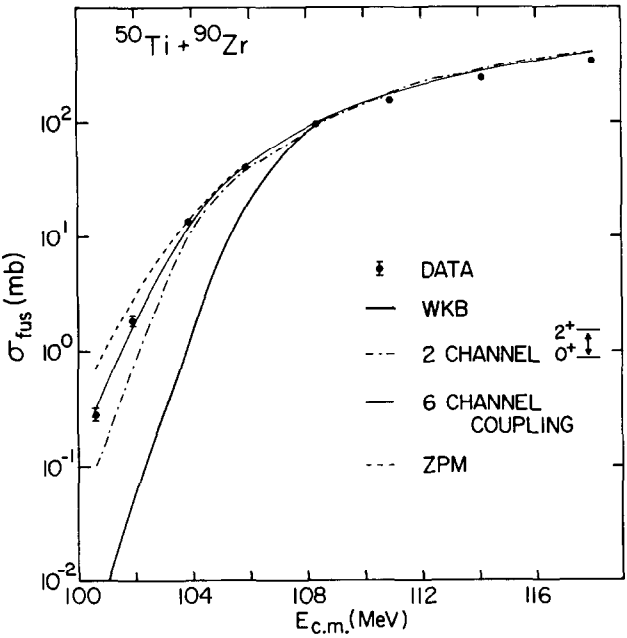

Fig. 1. Fusion cross sections for $^{50}Ti + ^{90}Zr$. The bold continuous curve is the result of the one-dimensional barrier penetration calculations. The two channel coupling result is shown by dash-dotted curve. The thin continuous curve is the result obtained by solving a 5-channel coupled equation. The 5 channels correspond to the first 5 excited vibrational states assumed in ^{50}Ti with a energy spacing of 1.55 MeV. The dashed curve is the prediction from ZPM. All calculations include the quadrupole Coulomb excitation and ignore the angular momentum transfer.

Rhoades-Brown *et al.*[3]) calculated subbarrier fusion cross sections for various medium heavy systems, using the coupled-channel code of PTOLEMY, which treats angular momentum algebra exactly. A few low-lying states were coupled to the relative motion with parameters extracted from the empirical spectra. It was found there that the subbarrier fusion was greatly enhanced compared with the one-dimensional penetration approximation, but was still underestimated, by orders of magnitude in some systems, for energies far below the Coulomb barrier. From our results for $^{50}Ti + ^{90}Zr$ we feel that if higher intrinsic couplings are treated correctly, one can reproduce the data in the coupled-channel model.

In the system $^{46}Ti + ^{90}Zr$, the predicted cross section with the empirical σ is too large. This suggests that the higher excitations in ^{46}Ti are not well approximated as harmonic overtones of the lowest excitation. With σ adjusted to a lower value, the cross section shape agrees very well with the data [14]), as may be seen in fig. 2. The ZPM agrees better with the coupled-channel calculation in the reaction because $\hbar\omega$ is smaller, only 0.8 MeV. In fig. 3 and fig. 4, we show the results for $^{50}Ti + ^{93}Nb$ and $^{46}Ti + ^{93}Nb$. The $\hbar\omega$ and σ for ^{93}Nb were taken as the averages of those for ^{92}Zr and ^{94}Kr. Again the agreement is good.

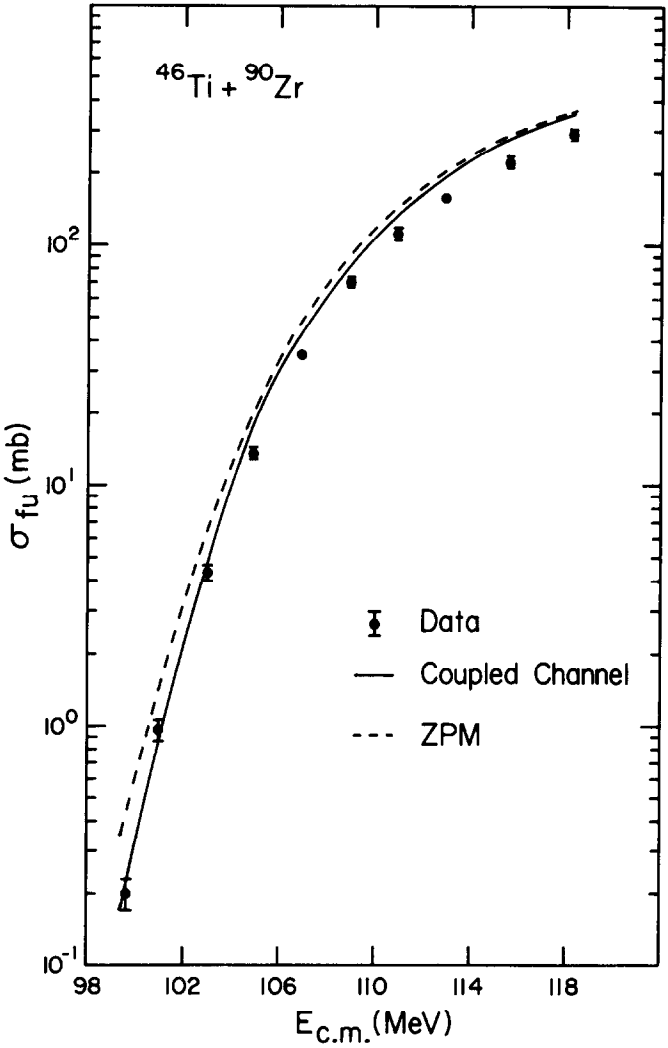

Fig. 2. Same plot as in fig. 1 but for ^{46}Ti+^{90}Zr. The parameters V_0, Ad and ΔR are same as those for ^{50}Ti+^{90}Zr. 0.89 MeV, the energy of the first excited state in ^{46}Ti, is used as the energy quanta for the vibrational mode. The σ is somehow 0.39 fm different from that quoted from the B(E2) measurement.

For heavier systems, fusion is inhibited at the configuration just inside the Coulomb barrier [15,16]). The critical projectile-target parameters for inhibition is given by [17])

$$K_{\mathrm{thr}} = (Z^2/A)_{\mathrm{eff\,thr}} = 35\{1 - 1.7826[(N_1 - Z_1 + N_2 - Z_2)/(A_1 + A_2)]^2\} \approx 35 .$$

The Ti+Zr and Nb systems have $K_{\mathrm{critical}} \approx 25$, well below the critical value. The next fusion reactions we consider are ^{81}Br+^{90,94}Zr and ^{90}Zr+^{90,94}Zr, measured by Beckerman *et al.* [18]). Here the K values range from 32 to 35, close to the critical value.

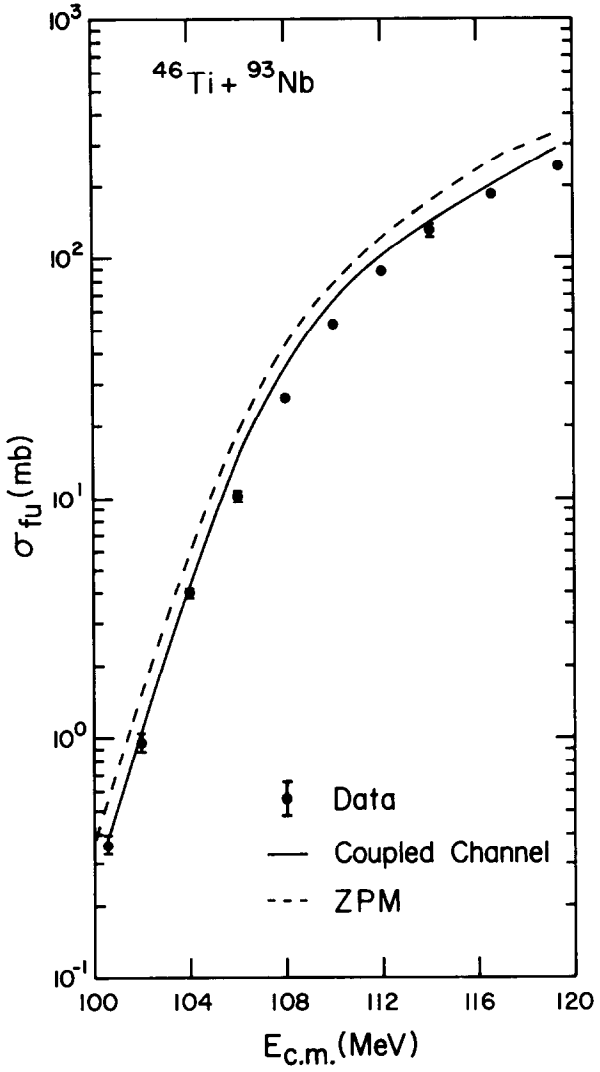

Fig. 3. Fusion cross sections for ^{46}Ti+^{93}Nb. The $\hbar\omega$ and σ for ^{93}Nb are taken as the average of those for ^{92}Zr and ^{94}Mo. The excitations in both ^{46}Ti and ^{93}Nb are combined into one mode with $\hbar\omega = \hbar\omega(^{46}\text{Ti}) = \hbar\omega(^{93}\text{Nb})$ and the σ equals to $\sqrt{\sigma^2(^{46}\text{Ti}) + \sigma^2(^{93}\text{Nb})}$. The number of channels coupled is 5.

In fig. 5 we plot the fusion cross section ratio of the ^{81}Br+^{94}Zr to the ^{81}Br+^{90}Zr. The effects of ^{90}Zr excitation is assumed small compared with that of ^{94}Zr, so we ignore it in the calculation. The σ and $\hbar\omega$ for ^{81}Br is obtained by subbarrier fusion fit for ^{81}Br+^{90}Zr. Then we can investigate the isotopic effects of Zr. As can be seen, the coupled-channel calculations including the excitation in ^{94}Zr (solid line) reproduce the data reasonably well. In contrast, the one-dimensional barrier treatment using a rescaled potential of the proximity form does not reproduce the relative

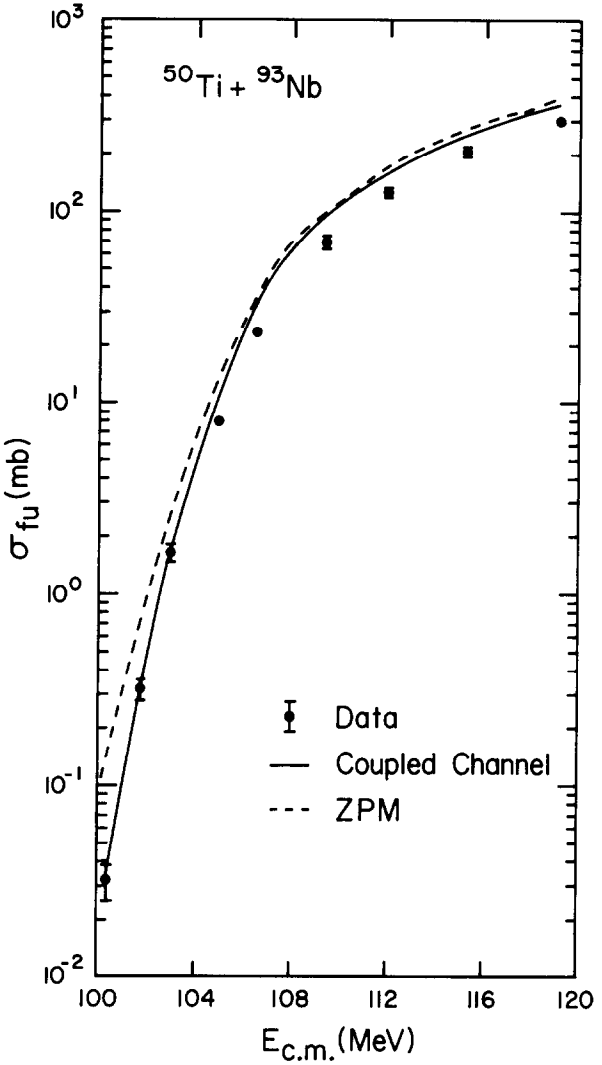

Fig. 4. Fusion cross sections for ^{50}Ti+^{93}Nb. In the coupled channel calculation, the $\hbar\omega$ is the average of those for ^{50}Ti and ^{93}Nb. The σ is $\sqrt{\sigma^2(^{50}\text{Ti}) + \sigma^2(^{93}\text{Nb})}$.

cross section. We do not show the absolute cross section because they are seriously overpredicted above the barrier.

In these heavy systems no extra-push energy is needed for fusion in the s-wave. However, starting at about $l = 26$ [ref. [17])], extra energy is needed beyond that to surmount the first potential barrier. Our method does not include the possibility of multiple fusion barriers, but this is not serious for the subbarrier region where only first a few partial waves contribute. Calculations above the barrier certainly need to include multiple barrier effects.

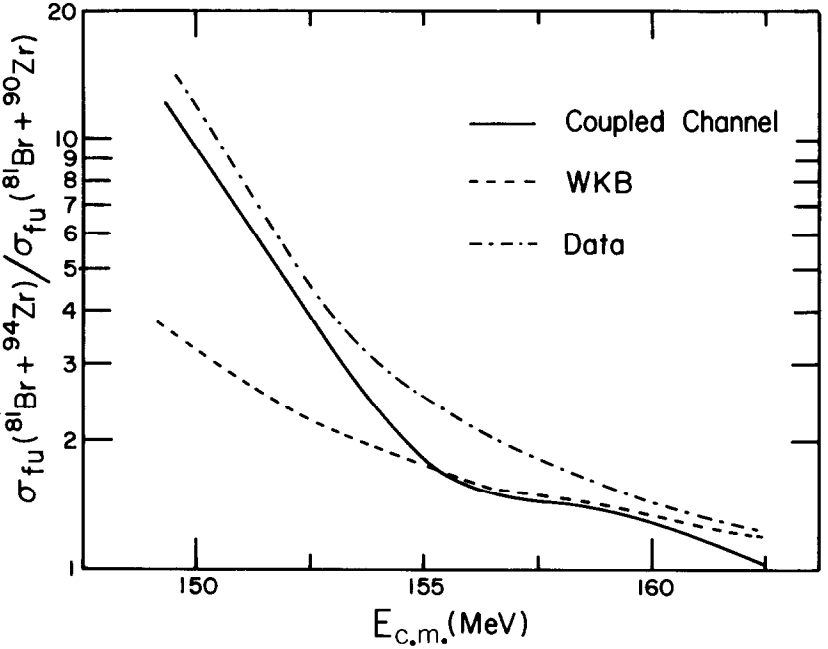

Fig. 5. The plot of the ratio of the fusion cross section for $^{81}Br+^{94}Zr$ to that for $^{81}Br+^{90}Zr$. The experimental data are the cross section for evaporation residue formation, instead of complete fusion.

We also calculated the fusion cross sections for the systems $^{90}Zr+^{90}Zr$ and $^{94}Zr+^{90}Zr$, measured in ref. [18]). The parameters V_0, a and ΔR are fixed by fitting the subbarrier fusion of $^{90}Zr+^{90}Zr$. But with these potential parameters the coupled channel calculations for $^{94}Zr+^{90}Zr$ underestimate the subbarrier fusion by about two orders of magnitude at lowest energy measured. We believe that the particle transfers in $^{94}Zr+^{90}Zr$ reactions may contribute to the subbarrier fusion significantly and account for the differences between the coupled channel calculations and the data [9]).

We conclude that subbarrier fusion for systems below the extra-push threshold can be quantitatively understood by a two-dimensional model. The collectivity of the lowest states is not sufficient to produce enough subbarrier enhancement, as the higher states in the harmonic spectrum are important at the lowest energies. This conclusion was also reached in a recent study of Ni+Ni subbarrier fusion [13]). For single magic nucleus we studied the harmonic approximation is very successful. For open shell nuclei, however, it somewhat overpredicts the collectivity. For heavier systems that require extra-push for fusion the simple two-dimensional model can reproduce the relative fusion cross section for different isotopes. The absolute fusion cross section, however, cannot be explained by the mocel.

We would like to thank Dr. P. Stelson and Dr. H. Esbensen for helpful discussions. This work is supported by National Science Foundation grant no. PHY 84-13287.

References

1) Lecture Notes in Physics **219** (1984), ed. S. Steadmen
2) A.B. Balantekin, S.E. Koonin and J.W. Negele, Phys. Rev. **C28** (1983) 1565
3) M.J. Rhoades-Brown, P. Braun-Munzinger, M. Prakash and S. Sen, *in* Lecture notes in physics, ed. S. Steadmen, vol. **219** (1984) p. 162
4) H. Esbensen, Nucl. Phys. **A352** (1981) 147
5) R. Pengo *et al.*, Nucl. Phys. **A411** (1983) 255
6) H. Esbensen, J.Q. Wu and G.F. Bertsch, Nucl. Phys. **A411** (1983) 275
7) H.J. Krappe *et al.*, Z. Phys. **A314** (1983) 23
8) S.C. Pieper, M.J. Rhoades-Brown and S. Landowne, Phys. Lett. **162B** (1985) 43
9) R.A. Broglia, C.H. Dasso, S. Landowne and G. Pollarolo, Phys. Lett. **133B** (1983) 34
10) O. Tanimura, J. Makowka and U. Mosel, Phys. Lett. **163B** (1985) 317
11) P.R. Christensen and A. Winther, Phys. Lett. **65B** (1976) 19
12) S. Landowne and H.H. Wolter, Nucl. Phys. **A351** (1981) 171
13) N. Takigawa and K. Ikeda, Tohoku Univ., preprint, 1985
14) P. Stelson, private communication
15) J.R. Nix and A.J. Sierk, Phys. Rev. **C15** (1977) 2072
16) W.J. Swiatecki, Phys. Scripta **24** (1981) 113; Nucl. Phys. **A376** (1981) 275
17) J.R. Birkelund and J.R. Huizenga, Ann. Rev. Nucl. Part. Sci. **33** (1983) 265
18) M. Beckerman, J. Wiggins, H. Aljuwair and M.K. Salomaa, Phys. Rev. **C29** (1984) 1938